# Spatial Distribution of LDOS in Cuprate Superconductors with Magnetic-Field-Induced Stripe Modulations

Hong-Yi Chen and C.S. Ting
*Texas Center for Superconductivity and Advanced Material, and Department of Physics, University of Houston, Houston, TX 77204*

A phenomenological model defined in a two dimensional lattice is employed to investigate the $d$-wave superconductivity and the competing antiferromagnetic order in cuprate superconductors. Near the optimally doped regime, we show that it is possible to induce the spin density wave (SDW) and the accompanying charge density wave (CDW) orders with stripe modulations by applying a magnetic field. The periods of the magnetic field induced SDW and CDW are $8a$ and $4a$, respectively. The spatial profiles of the local density of states (LDOS) at various bias energies have also been numerically studied. Near and beyond the energies of the vortex core states, we found that the LDOS may display the CDW stripe-like modulation throughout the whole magnetic unit cell. For energies closer to the zero bias, the stripes appear to be rather localized to the vortex. The intensity of the integrated spectrum of the LDOS shows that the strength of the stripe modulation is decaying away from the vortex core. This feature is in good agreement with STM experiments. The case for the magnetic-field induced SDW/CDW with 4-fold symmetry has also been studied.

PACS numbers: 74.25.Jb, 74.20.-z, 74.50.+r

In hole-doped cuprate superconductors, the interplay between the $d$-wave superconductivity (dSC) and antiferromagnetic (AF) order has been studied extensively in the literatures. Inelastic neutron scattering experiments showed the presence of incommensurate spin structures in $La_{2-x}Sr_xCuO_4$ (LSCO) [1] with a spatial periodicity $8a$ in the presence of a magnetic field. In addition, NMR imaging experiment on $YBa_2Cu_3O_{7-x}$ (YBCO) observed a strong AF fluctuation outside the vortex [2] indicating the possible existence of spin-density-wave (SDW) gap inside the vortex. A recent STM experiment by Hoffman *et al*. [3] seems to confirm the coexistence of the static charge modulation and the superconductivity on $Bi_2Sr_2CaCu_2O_8$ (BSCCO) under a magnetic field. The authors reported that a four unit cell checkerboard pattern is localized in a small region around the vortex, and its intensity is exponentially decaying away from the vortex core. All these experiments indicate that the AF fluctuations could be pinned by the vortex cores and they may form a static SDW/charge-density-wave (CDW) like modulations in certain samples of cuprate superconductors. Theoretically, a number of works proposed that the observed checkerboard patterns could be explained by the SDW order with the two-dimensional (2D) [4, 5, 6] or stripe [7, 8, 9] modulations. Both the 2D- and stripe-SDW orders induced by the magnetic field are well known to have the accompanying CDW modulations. In particularly, the checkerboard pattern has been attributed to the superposition of stripe modulations of the CDW [7, 10] oriented along $x$- and $y$- directions. In all these studies, the STM spectra obtained from the experiment have been directly interpreted in terms of the CDW order induced by the magnetic field. This is because that the conventional wisdom leads us to believe that the symmetry of the CDW order should be reflected in the STM spectra. On the other hand, the CDW order represents the charge density configuration in the ground state while the STM spectrum or the spatial distribution of the local density of states (LDOS) is determined by the behavior of the low-energy excitations in the system. It is therefore extremely interesting to know the difference between the CDW order and the spatial profile of the LDOS. This issue has not yet been addressed in the literature, and thus is the main purpose of the present paper.

The phonemenological $t - t' - U - V$ model defined in a 2D lattice and the Bogoliubov-de Gennes' equations will be used to numerically study the interplay between the $d$-wave superconductivity (dSC) and the competing AF order for samples close to the optimal doping. First the phase diagrams for the coexistence between these two orders as a function of $U/V$ in both zero and finite magnetic field are going to be examined. Two different values of $U/V$ will be chosen such that their magnitudes yield only the dSC when the magnetic field is zero. In the presence of a magnetic field, the $U/V(= 2.39)$ will give rise to a 2D SDW/CDW-like modulations while a stronger $U/V(= 2.44)$ would make the induced SDW/CDW to have one dimensional stripe-like structures. Then the spatial distributions of the LDOS as a function at various bias energies will be calculated and compared with those of the CDW. The spatial distributions of the integrated LDOS have also been obtained, and the result for $U/V = 2.39$ shows strong LDOS intensity near the vortex core and its distribution seems to be round, not the four-fold symmetry as expected for the CDW and dSC orders. The result for $U/V = 2.44$ shows that the stripe-like modulations are still existing but they are more localized near the vortex core and this is different from the CDW where the stripes are extended over the whole magnetic unit cell. These features are in good agreement

with the experiments of Pan *et al.* [11] and Hoffman *et al.* [3].

We start with an effective mean-field $t - t' - U$–V Hamiltonian in the mixed state by assuming that the on-site repulsion $U$ is responsible for the competing antiferromagnetism and the nearest-neighbor attraction $V$ causes the $d$-wave superconducting pairing.

$$\begin{aligned}\mathbf{H} &= -\sum_{\mathbf{ij}\sigma} t_{\mathbf{ij}} c^{\dagger}_{\mathbf{i}\sigma} c_{\mathbf{j}\sigma} + \sum_{\mathbf{i}\sigma} (U\langle n_{\mathbf{i}\bar{\sigma}}\rangle - \mu) c^{\dagger}_{\mathbf{i}\sigma} c_{\mathbf{i}\sigma} \\ &\quad + \sum_{\mathbf{ij}} (\Delta_{\mathbf{ij}} c^{\dagger}_{\mathbf{i}\uparrow} c^{\dagger}_{\mathbf{j}\downarrow} + \Delta^{*}_{\mathbf{ij}} c_{\mathbf{j}\downarrow} c_{\mathbf{i}\uparrow}) \,, \qquad (1)\end{aligned}$$

where $t_{\mathbf{ij}}$ is the hopping integral, $\mu$ is the chemical potential, and $\Delta_{\mathbf{ij}} = \frac{V}{2}\langle c_{\mathbf{i}\uparrow} c_{\mathbf{j}\downarrow} - c_{\mathbf{i}\downarrow} c_{\mathbf{j}\uparrow}\rangle$ is the spin-singlet $d$-wave bond order parameter. The Hamiltonian above shall be diagonalized by using Bogoliubov-de Gennes' (BdG) equations,

$$\sum_{\mathbf{j}}^{N} \begin{pmatrix} \mathcal{H}_{\mathbf{i}j\sigma} & \Delta_{\mathbf{ij}} \\ \Delta^{*}_{\mathbf{ij}} & -\mathcal{H}^{*}_{\mathbf{ij}\bar{\sigma}} \end{pmatrix} \begin{pmatrix} u^{n}_{\mathbf{j}\sigma} \\ v^{n}_{\mathbf{j}\bar{\sigma}} \end{pmatrix} = E_n \begin{pmatrix} u^{n}_{\mathbf{i}\sigma} \\ v^{n}_{\mathbf{i}\bar{\sigma}} \end{pmatrix} \,, \qquad (2)$$

where $\mathcal{H}_{\mathbf{ij}\sigma} = -t_{\mathbf{ij}} + (U\langle n_{\mathbf{i}\sigma}\rangle - \mu)\delta_{\mathbf{ij}}$. Here, $t_{\mathbf{ij}} = \langle t_{\mathbf{ij}}\rangle e^{i\varphi_{\mathbf{ij}}}$ . The Peierl's phase factor $\varphi_{\mathbf{ij}} = \frac{\pi}{\Phi_0}\int_{r_{\mathbf{i}}}^{r_{\mathbf{j}}} \mathbf{A}(\mathbf{r})\cdot d\mathbf{r}$ , with the superconducting flux quantum $\Phi_0 = hc/2e$. Within the Landau gauge $\mathbf{A}(\mathbf{r}) = (-By, 0, 0)$, each magnetic unit cell can accommodate two superconducting vortices. The vortex carries a flux quantum $\Phi_0$ and locate at the center of a square area containing $N_x/2 \times N_y$ sites with $N_x = 2 \times N_y$. Here, we choose the nearest-neighbor hopping $\langle t_{\mathbf{ij}}\rangle = t = 1$ and the next-nearest-neighbor hopping $\langle t_{\mathbf{ij}}\rangle = t' = -0.25$ to match the curvature of the Fermi surface for most cuprate superconductors. The exact diagonalization method to self-consistently solve BdG equations with the periodic boundary conditions is employed to get the $N$ positive eigenvalues ($E_n$) with eigenvectors $(u^{n}_{\mathbf{i}\uparrow}, v^{n}_{\mathbf{i}\downarrow})$ and negative eigenvalues ($\bar{E}_n$) with eigenvectors $(-v^{n*}_{\mathbf{i}\uparrow}, u^{n*}_{\mathbf{i}\downarrow})$. The self-consistent conditions are

$$\begin{aligned}\langle n_{\mathbf{i}\uparrow}\rangle &= \sum_{n=1}^{2N} |\mathbf{u}^{n}_{\mathbf{i}}|^2 f(E_n) \,,\ \langle n_{\mathbf{i}\downarrow}\rangle = \sum_{n=1}^{2N} |\mathbf{v}^{n}_{\mathbf{i}}|^2 [1 - f(E_n)] \,, \\ \Delta_{\mathbf{ij}} &= \sum_{n=1}^{2N} \frac{V}{4} (\mathbf{u}^{n}_{\mathbf{i}} \mathbf{v}^{n*}_{\mathbf{j}} + \mathbf{v}^{n*}_{\mathbf{i}} \mathbf{u}^{n}_{\mathbf{j}}) \tanh(\frac{\beta E_n}{2}) \,, \qquad (3)\end{aligned}$$

where $\mathbf{u}^{n}_{\mathbf{i}} = (-v^{n*}_{\mathbf{i}\uparrow}, u^{n}_{\mathbf{i}\uparrow})$ and $\mathbf{v}^{n}_{\mathbf{i}} = (u^{n*}_{\mathbf{i}\downarrow}, v^{n}_{\mathbf{i}\downarrow})$ are the row vectors, and $f(E) = 1/(e^{\beta E} + 1)$ is Fermi-Dirac distribution function. Since the calculation is performed near the optimally doped regime, the filling factor, $n_f = \sum_{\mathbf{i}\sigma}\langle c^{\dagger}_{\mathbf{i}\sigma} c_{\mathbf{i}\sigma}\rangle / N_x N_y$, is fixed to be 0.85, i.e., the hole doping $\delta = 0.15$. Each time when the on-site repulsion $U$ is varied, the chemical potential $\mu$ needs to be adjusted .

In the limit of $U/V \ll 1$, the system is in the state of pure dSC. In the opposite limit $U/V \gg 1$, the system is the SDW states. However, the most anomalous properties of cuprate superconductors do not correspond to these extreme limits, but are in the intermediate case where both the SDW and the SC may coexist. In order to simplify our discussion of the ratio of $U$ to $V$, we set $V = 1.0$. In Fig. 1(a), without the magnetic field, $B = 0$, the staggered magnetization ($M_{\mathbf{i}}$) or the SDW shows either the stripe modulation or the uniform distribution with $M_{\mathbf{i}} = 0$ in the background of dSC depending upon the magnitude of $U$. For $U > U_{c1}$, the staggered magnetization exhibits the stripe modulation with $8a$ as its periodicity (a is the lattice constant). On the other hand, for the $U$ less than $U_{c1}$, it shows the uniform distribution which is equivalent to the state of pure dSC. It is important to point here that a two-dimensional (2D) SDW modulation can never be obtained when $B = 0$ in the present self-consistent calculation. The transition between the SDW-stripe modulation and the uniform distribution is discontinuous. In Fig. 1(b), under an applied magnetic field, the staggered magnetization (solid line) displays the stripe modulation, the two dimensional SDW, or the uniform distribution depending on $U$. As $U$ is greater than $U_{c1}$, the stripe modulation existed in the zero field would be *slightly enhanced* under a magnetic field (Stripe$_{(I)}$). In the region of $U_{c2} < U \le U_{c1}$, the field induced staggered magnetization shows a stripe modulation which disappears in the zero field (Stripe$_{(II)}$). For $B \neq 0$, the transition between stripe$_{(I)}$ and stripe$_{(II)}$ is not apparent and only the slope shows a weak discontinuity. When $U \le U_{c2}$, the field induced AF order changes from the stripe-like to a 2D SDW. If $U$ goes down far

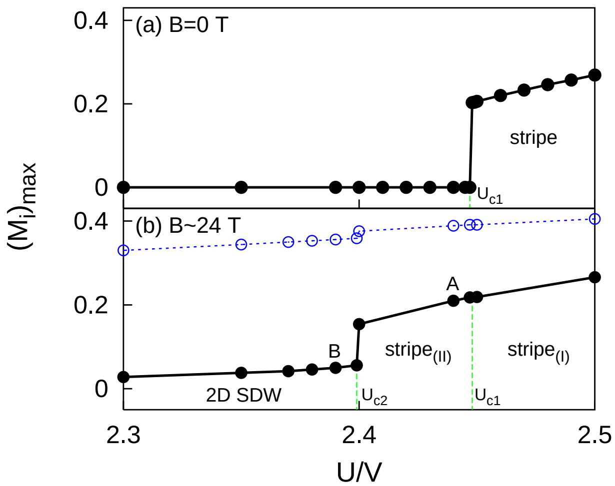


FIG. 1: The maximum value of the staggered magnetization in the zero-field (a), and in the finite field (b). In (b), the open circle and the solid circle represent the (maximum) staggered magnetization at the center of the vortex core and away from the vortex cores, respectively. Stripe$_{(I)}$ is the region where the stripe modulations are intrinsic and stripe$_{(II)}$ corresponds to the region where the stripe modulations are field-induced. The size of the unit cell is $N_x \times N_y = 48 \times 24$ correspoding to a magnetic field $B \sim 24T$.

below 2.3, the AF order could be completely suppressed both inside or outside the vortex cores. The transition between the stripe modulation and the 2D SDW is of the first order. Accompanying the stripe-like AF order, there also exists a CDW with the stripe modulation of the period $4a$. At the same time the dSC order parameter also acquires a CDW-like stripe modulation. In Fig. 1(b), the staggered magnetization (open circles) at the vortex core center seems to be weakly $U$ dependent. In the following, $U = U_A = 2.44$ and $U = U_B = 2.39$ are chosen for our study of the LDOS. Both of these $U$ values would not generate the SDW/CDW order for nearly optimally doped cuprate superconductors when $B = 0$. In order to understand the characteristics between the two cases, we start with the LDOS formula

$$\rho_{\mathbf{i}}(E) = -\frac{1}{M_x M_y} \sum_{n,\mathbf{k}}^{2N} \{ \left|\mathbf{u}_{\mathbf{i}}^{n,\mathbf{k}}\right|^2 f'(E_{n,\mathbf{k}} - E) + \left|\mathbf{v}_{\mathbf{i}}^{n,\mathbf{k}}\right|^2 f'(E_{n,\mathbf{k}} + E) \} , \quad (4)$$

where $\rho_{\mathbf{i}}(E)$ is proportional to the local differential tunneling conductance as measured by STM experiment, and the summation is averaged over $M_x \times M_y$ wavevectors in first Brillouin Zone.

The LDOS as a function of energy have been numerically calculated at the vortex core center (solid line) and at site far away from the vortex (dashed line) for $U_A$ and $U_B$, the results are respectively given in Fig. 2(a) and 2(b). There the spatial profiles of the field induced CDW modulations are presented in Fig. 2. For $U_A$, the field induced CDW has the stripe-like structure which extends over the whole magnetic unit cell with a period $4a$ while for $U_B$, the CDW modulation becomes two dimensional with four-fold symmetry.

Since the SDW gap develops inside the vortex core, the resonance peak appeared in the LDOS [13] near the zero bias in a pure dSC at the core center is suppressed and splits into two peaks [14]. This feature can be seen in the Fig. 2. Furthermore, STM experiments on YBCO [12] and BSCCO [11] measured the double peaks structure within the maximum superconducting gap. The states associated with these two peaks have been referred as the vortex core states. Here we would like to point out that our results for the LDOS seem to agree better with YBCO [12] than BSCCO [11]. In Fig. 2, those vortex core states with negative energies are centered at $E_A = -0.19$ with a width $\Delta E_A = 0.08$ and $E_B = -0.21$ with $\Delta E_B = 0.04$ for $U_A$ and $U_B$, respectively.

Because the energy dependence of the LDOS at the vortex center does not make any clear distinction between $U_A$ and $U_B$, we examine the spatial profile of the LDOS at various energies and look for their differences. In Fig. 3, the LDOS maps (the spatial distribution of the LDOS), which are the LDOS with fixed energy at each site of the magnetic unit cell, have been calculated at

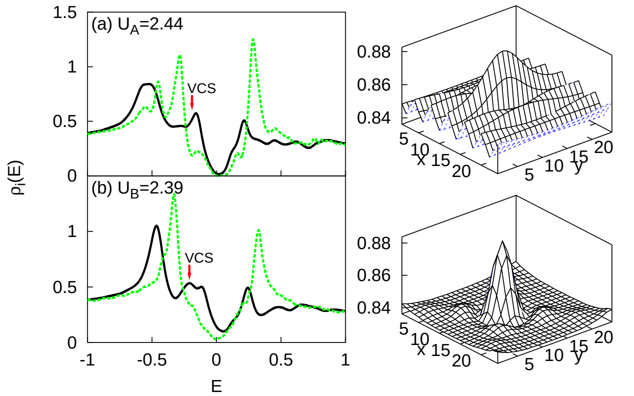


FIG. 2: The LDOS as a function of energy, left panel, at the vortex core center for (a) $U_A = 2.44$, (b) $U_B = 2.39$. The solid line is at the vortex core center, and the dash line is at the site far away the vortex. The arrow points the vortex core states (VCS). The spatial profiles of the corresponding CDW are shown in the right panels of Fig. 2. The wavevectors in first Brillouin Zone are $M_x \times M_y = 24 \times 24$.

energies ranging from 0.0 to $-0.4$ with $\delta E = 0.01$ decrement. For $U_A$, as the energy far below the vortex core states (VCS) and close to the zero bias, the pattern in Fig. 3(a) shows that the stripe structure with periodicity $4a$ is strongly localized near the vortex core, and its strength drops dramatically away from the vortex. When the energy near the VCS, such as Fig. 3(b), the stripe modulation in the LDOS extends over the whole unit cell, similar to the feature in CDW in Fig. 2(a). If the bias voltage goes above or becomes more negative than the VCS, such as Fig. 3(c), the stripe modulation is still extensive, but the intensities inside the vortex core are depressed than those outside the vortex core. Thus the STM spectra or the LDOS do not have all the features of the CDW.

For $U_B$, as the energy far below the vortex core states (VCS) [see Fig. 3(e)], the LDOS pattern shows a *round* bump with the size of a vortex core. When the energy is near the VCS, such as in Fig. 3(f), the LDOS shows a distribution with rather weak oscillations, and its feature is not quite similar to that of the CDW in Fig. 2(b). If the energy is above the VCS, such as that in Fig. 3(g), the modulation here clearly displays the pattern with 4-fold symmetry. However, the STM images obtained experimentally [3] are results of integrating the spectral density between energies $E_1$ and $E_2$, which is defined as

$$S(E_1, E_2) = \sum_{E_1}^{E_2} \rho_{\mathbf{i}}(E) \delta E , \quad (5)$$

There, [3] $E_1$ is taken to be 0 and $E_2$ has been set near the energy of the VCS below the chemical potential. In Fig. 3(d), the integrated spectrum $S(0.0, -0.23)$ of the LDOS is obtained by summing the LODS from $E_1$ to $E_2$ with an energy spacing 0.01. It shows that the inten-

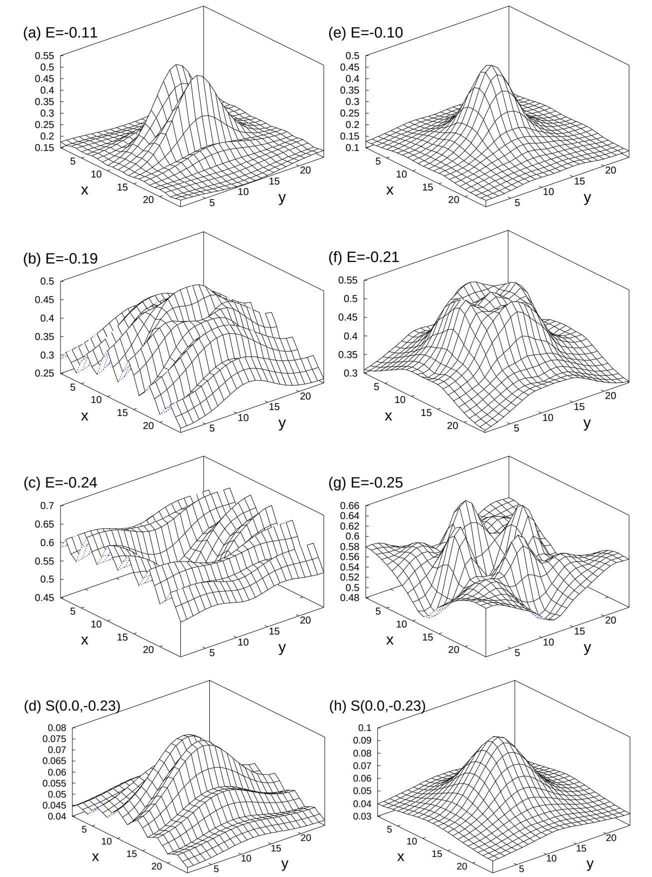


FIG. 3: The LDOS maps are at energies (a) and (e)-close to the zero bias, (b) and (f)-near the VCS, and (c) and (g) above the VCS. The integrated spectrum of LDOS $S(E_1, E_2)$ of (d) and (h) are from the Fermi energy to the upper bound of the VCS, i.e., $S(0.0, -0.23)$. The left and right panel are for $U_A = 2.44$ and $U_B = 2.39$, respectively. The wavevectors in first Brillouin Zone are $M_x \times M_y = 6 \times 6$.

sity of the stripe modulations is dominantly concentrated near the vortex core and decays rapidly when away from the vortex. This feature originates from the behaviors of the LDOS at energies with magnitudes smaller than those of the VCS [see Fig. 3(a)]. Since the LDOS maps display the properties of the $eigenfunction$ at the energy $E$, the checkerboard pattern observed by the experiments could be explained in terms of the superposition of the degenerate eigenfunctions describing the stripe modulations along $x$- and $y$- directions. All these behaviors are in good agreement with the experiment [3]. We expected that the qualitative features obtained for $U_A$ should still remain even if $U > U_{c1}$ and the stripe phase is intrinsic not magnetic field induced (see Fig. 1). In Fig. 3(h), the integrated spectrum of the LDOS for $U_B$ exhibits a *round* bump over the vortex core region which is different from that of the CDW as shown in Fig. 2(b). For a sample without the stripe modulations, the profile of the integrated LDOS near the vortex core seems to be rather *round* and does not possess the strong 4-fold symmetry as expected for a dSC [14]. This feature is also consistent with the STM experimental measurements [11] provided that the samples used there is different from that of [3].

In conclusion, we have numerically investigated the interplay between the dSC and the competing SDW/CDW orders by varying the strength of $U/V$ for samples close to the optimal doping. For finite field, we show that both stripe-like and two dimensional SDW/CDW orders, depending on the magnitude of $U/V$, may be induced in the background of the dSC. We in particular calculate the spatial distribution of the LDOS with and without the SDW/CDW stripes at various bias energies. We point out that the checkerboard pattern near the vortex core observed by Hoffman *et al.* [3] could be interpreted in terms of superposition of the field-induced $x$- and $y$- oriented stripes. The obtained features of our integrated LDOS with stripes and without stripes [see Figs. 3(d) and 3(h)] are in good agreement with the STM experiments [3, 11]. It is well known that the theoretically obtained profiles for the dSC order parameters together with the induced 2D SDW/CDW modulations near the vortex core exhibit a clear 4-fold symmetry. This symmetry, however, so far has not been confirmed by existing STM measurements. Here, we predict that this 4-fold symmetry should be more easily detectable when the bias is placed beyond the energies of the vortex core states [see Fig. 3(f)].

**Acknowledgements**: We wish thank S.H. Pan for useful comments and suggestions. This work is supported by the Texas Center for Superconductivity and Advanced Material and Department of Physics at the University of Houston, and by the grant of the Robert A. Welch Foundation.

[1] B. Lake, G. Aeppli, K.N. Clausen, D.F. McMorrow, K. Lefmann, N.E. Hussey, N. Mangkorntong, M. Mohrara, H. Takagi, T.E. Mason, and A. Schroder, Science **291**, 1759 (2001).

[2] V.F. Mitrovic, E.E. Sigmund, M. Eschrig, H.N. Bachman, W.P. Halperin, A.P. Reyes, P. Kuhns, and W.G. Moulton, Nature **413**, 501 (2001).

[3] J.E. Hoffman, E.W. Hudson, K.M. Lang, V. Madhavan, S.H. Pan, H. Eisaki, S. Uchida, and J.C. Davis, Science **295**, 466 (2002).

[4] Han-Dong Chen, J.P. Hu, S. Capponi, E. Arrigoni, and S.C. Zhang, Phys. Rev. Lett. **89**, 137004 (2002).

[5] A. Polkovnikov, M. Vojta, and S. Sachdev, Phys. Rev. B **65**, 220509 (2002).

[6] J.X. Zhu, I. Martin, and A.R. Bishop, Phys. Rev. Lett. **89**, 067003 (2002).

[7] Y. Chen, Hong-Yi Chen, and C.S. Ting, Phys. Rev. B **66**, 104501 (2002).

[8] D. Podolsky, E. Demler, K. Damle, and B.I. Halperin, Phys. Rev. B **67**, 094514 (2003).

[9] M. Ichioka, M. Takigawa, and K. Machida, J. Phys. Soc. Jpn. **70**, 33 (2001).

[10] S.A. Kivelson, E. Fradkin, V. Oganesyan, I.P. Bindloss, J.M. Tranquada, A. Kapitulnik, and C. Howald, cond-mat/0210683.
[11] S.H. Pan, E.W. Hudson, A.K. Gupta, K.-W. Ng, H. Eisaki, S. Uchida, and J.C. Davis, Phys. Rev. Lett. **85**, 1536 (2000).
[12] I. Maggio-Aprile, Ch. Renner, A. Erb, E. Walker, and Ø. Fischer, Phys. Rev. Lett. **75**, 2754 (1995).
[13] Y. Wang and A.H. MacDonald, Phys. Rev. B **52**, R3876 (1995).
[14] Jian-Xin Zhu and C.S. Ting, Phys. Rev. Lett. **87**, 147002 (2001).